Egyptian Journal of Petroleum (2016) xxx, xxx–xxx

HOSTED BY

ELSEVIER

Egyptian Petroleum Research Institute

Egyptian Journal of Petroleum

www.elsevier.com/locate/egyjp
www.sciencedirect.com

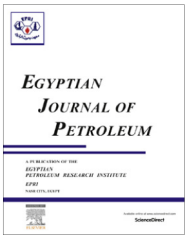

FULL LENGTH ARTICLE

A comprehensive study of ondansetron hydrochloride drug as a green corrosion inhibitor for mild steel in 1 M HCl medium

Vengatesh G., Karthik G., Sundaravadivelu M. *

Department of Chemistry, Gandhigram Rural Institute-Deemed University, Gandhigram, Tamilnadu 624302, India

Received 28 April 2016; revised 11 June 2016; accepted 16 October 2016

KEYWORDS

Mild steel;
Acid medium;
Adsorption isotherm;
Quantum chemical study;
EIS;
AFM

Abstract The inhibiting action against the corrosion of mild steel by ondansetron hydrochloride (ODSH) drug was studied, using various studies such as weight loss, electrochemical impedance spectroscopy, potentiodynamic polarization measurement, scanning electron microscopy (SEM), energy dispersive X-ray spectroscopy (EDX), atomic force microscopy (AFM), FT-IR spectroscopy and reactivity of molecule is studied using quantum chemical calculation. The result shows that ondansetron hydrochloride (ODSH) gives better inhibition on mild steel. The value of activation energy (E_a) and various thermodynamic parameters such as adsorption equilibrium constant (K_{ads}), free energy of adsorption (ΔG^0_{ads}), adsorption enthalpy (ΔH_{ads}) and adsorption entropy (ΔS_{ads}) was calculated and discussed. The adsorption of ODSH on mild steel surface obeys the Langmuir adsorption isotherm. Potentiodynamic polarization measurement reveals that ODSH acts as a mixed-type inhibitor. Electrochemical impedance spectroscopy (EIS) spectra exhibit one capacitive loop indicating that, the corrosion reaction is controlled by charge transfer process. SEM, EDX, AFM, FT-IR conforms to the protective film formation. Quantum chemical calculation was calculated and discussed, and it supports the results.

1. Introduction

Corrosion protection studies of iron and its alloys play a vital role due to their wide range of industrial applications especially in the petroleum industry and power plants [1]. An acid solution was generally used for the removal of undesirable scale and rust in several industrial processes, hydrochloric and sulfuric acids are widely used in these processes [2]. A number of methods have been used to reduce the corrosion of metal such as cathodic protection, metal plating, coatings, inhibitors, etc.; the use of inhibitors is one of the most useful methods for the protection of material against corrosion. Most well-known acid inhibitors are organic compounds because they contain polar functional groups (nitrogen, sulfur, oxygen and phosphorus) and aromatic π electrons, they easily contact to the metal surface and form a protecting layer [3–12]. The applicability of organic compound as corrosion inhibitors for

* Corresponding author.
E-mail addresses: vengateshche@gmail.com (G. Vengatesh), karthik.gtn@gmail.com (G. Karthik), msundargri@gmail.com (M. Sundaravadivelu).

Peer review under responsibility of Egyptian Petroleum Research Institute.

http://dx.doi.org/10.1016/j.ejpe.2016.10.011

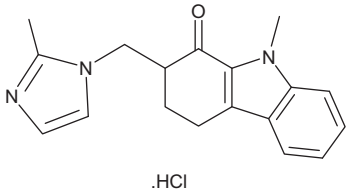

Figure 1 Structure of ondansetron hydrochloride.

metals in the acid medium have been recognized for a long time [13–17]. They exert inhibition action through adsorption of the inhibitor on the metal surface, they block the corrosion active sites by removal of the water molecule and forming a protective layer on the metal surface; this is due to a decrease in the corrosion rate of metal. The adsorption behavior of organic molecules on the metal surface depend on the nature of the metal surface, electrochemical potential of the metal and solution interface, the number of adsorption active centers in the molecule, the size of the molecule, the mode of adsorption and their charge density [18,19].

Up to now, many pharmaceutically active compounds are used as the corrosion inhibitors, for metallic corrosion studies. Some of the compounds are given; Cefatrexyl [20], Antifungal drugs (clotrimazole, fluconazole) [21], Cefotaxime sodium [22], Cefalexin [23], Ketosulfone [24], Rodamine azosulfa drug [25], Esomeprazole [26], Sulfa drugs (e.g. sulfaguanidine, sulfamethazine, sulfamethoxazole and sulfadiazine) [27], Streptomycin [28], Cefazolin [29], Mebendazole [30], Pheniramine [1], Cloxacillin [31] and Cefixime [32].

The main objective here is to investigate the corrosion inhibition process of mild steel in one molar hydrochloric acid using ODSH. The IUPAC name of ondansetron hydrochloride is 9-methyl-3-(2-methyl-imidazol-1-ylmethyl)-1,2,3,9-tetrahydro-carbazol-4-one (Fig. 1). The Mebendazole molecular formula of ODSH is $C_{18}H_{20}N_3OCl$ and the molecular weight is 329.81 g/mol. Furthermore, ODSH is easily available, environmentally friendly and the most important it is non-toxic in nature. It is pharmaceutically used to prevent nausea and vomiting treatment. In view of these favorable characteristics, we are choosing ODSH for the corrosion inhibitor study.

2. Materials and methods

2.1. Materials

The mild steel sample used for the study contains the following composition (in wt.%) 0.104% C, 0.58% Mn, 0.035% P, 0.026% S and the remainder Fe.

2.2. Inhibitor

The inhibitor was purchased from Mankind Pharmacy Pvt. Ltd. (brand name vomikind) New Delhi. It contains three N atom, one O atom, and a heterocyclic ring. These atoms can easily protonate in acid medium and protect the metal surface by forming a protective film in metal/solution interface.

2.3. Solutions

The aggressive solution of 1 M HCl was prepared by dilution of AR grade, 35% HCl with double distilled water. The concentration range of inhibitor was taken in 50–300 ppm. The stock solution is prepared using this relation 1000 ppm = 1000 mg made in 1 l. Stock solution is used to making the different concentrations of inhibitor (50–300 ppm) are prepared based on volumetric law ($V_1N_1 = V_2N_2$).

2.4. Weight loss measurements

A rectangular steel plate had been used in the weight loss study. The size of the steel that is 3.5 × 1.5 × 0.2 cm was cut with a small hole on the upper edge of the specimen. It is mechanically polished with different grades of emery papers 1/0–1/7 and then washed with acetone. After the washing, the specimens were weighed accurately using digital balance and the specimens were immersed in 100 ml 1 M HCl without and with various concentrations of ODSH using glass hooks. The inhibitor concentrations used in the weight loss study are in the ranges of 50–300 ppm. All the aggressive acid solutions were kept open to air. After immersion for 3 h, the specimens were taken out, washed with a bristle brush under running water in order to remove the corrosion product, dried with the hot air stream, and re-weighed accurately to calculate weight loss. In this, experiments were carried out in triplicate method to get good reproducibility results in the measurement. The standard deviation value among parallel triplicate experiments was found to be lower than 5%, indicating good reproducibility. Then the tests were repeated at different temperatures. The temperature study was carried out at 303–333 K. The corrosion rate (CR) is calculated by the following equation [33].

$$CR = \frac{W}{St} \tag{1}$$

where W is the average weight loss of three rectangular steels, S is the total area of rectangular steel, and t is immersion time (3 h). With the calculated corrosion rate, the inhibition efficiency (IE%) and surface coverage (θ) were calculated as follows [34].

$$IE\ \% = \left[\frac{W_o - W_i}{W_o}\right] \times 100 \tag{2}$$

$$\theta = \left[\frac{W_o - W_i}{W_o}\right] \tag{3}$$

where W_0 is the corrosion rate in the absence of inhibitor and W_i is the corrosion rate in the presence of inhibitor.

2.5. Adsorption isotherm and thermodynamic parameters

In order to learn about the mode of adsorption of ODSH on the metal surface in 1 M HCl at different temperatures, attempts were made to fit experimental data with various adsorption isotherms. Using these data, thermodynamic parameters were calculated using standard equations.

Please cite this article in press as: G. Vengatesh et al., A comprehensive study of ondansetron hydrochloride drug as a green corrosion inhibitor for mild steel in 1 M HCl medium, Egypt. J. Petrol. (2016), http://dx.doi.org/10.1016/j.ejpe.2016.10.011

2.6. Electrochemical measurements

Two electrochemical techniques mainly used in the corrosion inhibitor study namely, Tafel polarization and (EIS) were used to study the inhibition behavior of inhibitor. All electrochemical measurements were carried out using a CHI 760D electrochemical analyzer model. These electrochemical experiments were carried out in the conventional three-electrode cell with a platinum foil as the counter electrode (CE), a saturated calomel electrode (SCE) as the reference electrode and 1 cm^2 of mild steel as a working electrode. The working electrode was polished as mentioned above. Before measurement, the electrode was immersed in a blank solution to carry out open circuit potential (OCP) for 45 min to be sufficient to attain a stable state. Each experiment was repeated three times to check the reproducibility.

The EIS measurements were carried out using an AC signal of 0.01 V amplitude of the frequency spectrum from 100 kHz to 0.01 Hz at the predetermined open circuit potential (OCP). The inhibition efficiency (IE%) and surface coverage (θ) were calculated from the electrochemical impedance spectra by the following equation [35]:

$$\text{IE } (\%) = \left[\frac{R_{ct}^{i} - R_{ct}^{o}}{R_{ct}^{i}}\right] \times 100 \quad (4)$$

$$\theta = \left[\frac{R_{ct}^{i} - R_{ct}^{o}}{R_{ct}^{i}}\right] \quad (5)$$

where R_{ct}^{i} and R_{ct}^{o} are the charge transfer resistance values with and without ODSH respectively. The inhibitor efficiency and surface coverage (θ) were calculated from the polarization curves by the following equation [34]:

$$\text{IE } (\%) = \left[\frac{I_{corr}^{o} - I_{corr}^{i}}{I_{corr}^{o}}\right] \times 100 \quad (6)$$

$$\theta = \left[\frac{I_{corr}^{o} - I_{corr}^{i}}{I_{corr}^{o}}\right] \quad (7)$$

where I_{corr}^{i} and I_{corr}^{o} are the corrosion current densities with and without inhibitor, respectively.

2.7. Surface morphology

The mild steel surface was examined by making photographs of the surface in the absence and presence of the optimum concentration of ODSH (300 ppm) separately for after three hrs of immersion. The scanning electron microscopy (SEM) VEGA3-TESCAN model and atomic force microscopy (AFM) NTMDT model were used for this purpose. The FT-IR spectra were recorded using JASCO 460 PLUS spectrometer over the range of 400–4000 cm^{-1} with the resolution of 4 cm^{-1}, using the KBr disk technique.

2.8. Computational details

All geometry optimizations and quantum calculations were performed using density functional theory (DFT) and utilizing the 6–31 + G (d, p) basis sets. DFT/B3L YP is recommended for the study of chemical reactivity and selectivity in terms of the frontier molecular orbital theory [35].

3. Result and discussion

3.1. Weight loss method

The weight loss method was used to determine the metal weight loss and efficiency of inhibitor, which is a simple and traditional method [35,36]. In this study, the reproducibility results were obtained and the inhibition efficiency values were determined from original and two duplicate sample. This three-sample result is very precise (±2%). The inhibition efficiency of the ODSH is shown in Table 1. From the Table 1, it is clear that when the concentration of the ODSH increases, the corrosion rate decreases and the percentage of IE%

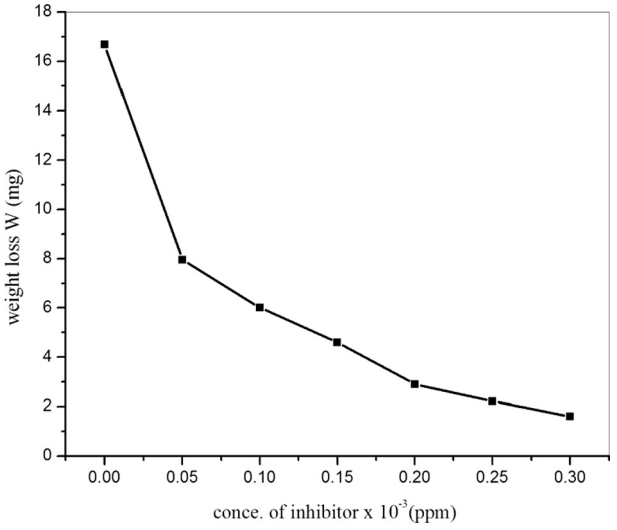

Figure 2 Relationship between weight loss vs concentration of inhibitor.

Table 1 Weight loss values of various concentrations of ODSH in 1 M HCl.

Concentration (ppm)	Weight loss (mg cm^{-2})	Corrosion rate (mm y^{-1})	Surface coverage (θ)	IE (%)
Blank	16.67	39.69	–	–
50	7.96	18.95	0.5224	52.24
100	6.01	14.30	0.6394	63.94
150	4.60	10.95	0.7240	72.40
200	2.91	6.92	0.8254	82.54
250	2.22	5.28	0.8668	86.68
300	1.60	3.80	0.9040	90.40

increases. The results are graphically presented in Figs. 2 and 3.

Fig. 2 shows that metal weight decreases gradually when increasing the concentration of inhibitor in 1 M HCl solution at 30 °C because the adsorption amount and coverage of inhibitor on mild steel surface increases with increasing the concentration of ODSH [37]. In Fig. 3 when the concentration of ODSH increases, inhibitor efficiency increases and it clearly indicates that adsorption process occurs on the metal surface.

The IE% increases sharply with an increase in the concentration of inhibitor; while a further increase in the concentration of inhibitor (above 300 ppm), there is no appreciable change in IE%. This is because the inhibitor in 300 ppm covers all active sites of metal so above this concentration, there is no change in IE% and maximum efficiency is 90% at 300 ppm.

3.1.1. Effect of inhibitor concentration

The value of IE% and CR obtained from weight loss method at various concentrations of ODSH in 1 M HCl, by immersing the mild steel plates in inhibitor solution in 3 h is summarized in Table 1. The IE% increased from 55.68 to 90.41% with the addition of 50–300 ppm of ODSH, and the results are shown in Fig. 3. The CR decreased from 39.69 to 3.80 mm y^{-1} with the addition of 50–300 ppm of ODSH.

The CR and IE% are inversely proportional to one another. The increase in IE% and a decrease in CR may be due to an increase in absorption and the increase in coverage of ODSH on the mild steel surface with increasing concentration of inhibitor [37]. It is clear that ODSH showed good inhibition for mild steel corrosion in 1 M HCl solution because the inhibitor molecule is made of planar aromatic ring and the imidazole ring-containing O, N atoms and π-electrons [30].

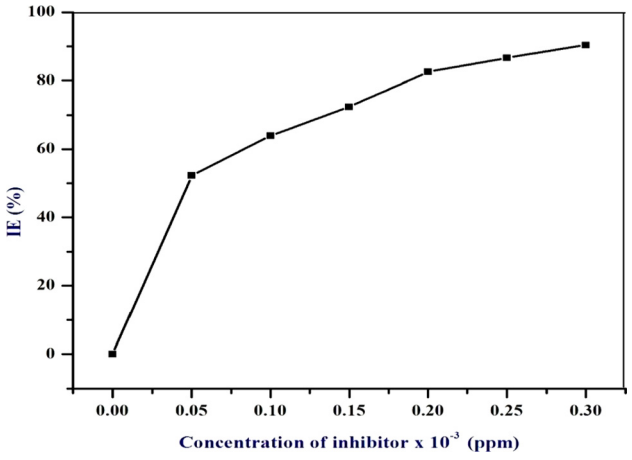

Figure 3 Relationship between inhibition efficiency vs concentration of inhibitor.

3.1.2. Effect temperature

The weight loss of the mild steel in 1 M HCl in the absence and presence of various concentrations of ODSH at different temperatures from 303 K to 333 K was determined and the results are exhibited in Table 2. As the concentration of inhibitor increases and inhibition efficiency also increases, but when the temperature increases the inhibitor efficiency decreases as shown in Fig. 4. This is because at a high temperature, the hydrogen evolution increases on the metal surface and desorption of the thin film takes place and so inhibitor efficiency decreases. When the temperature increases the corrosion rate is increased linearly and it is shown in Table 2. It clearly indicates that temperature mainly influences the desorption of adsorbed inhibitor on the metal surface.

3.1.3. Adsorption isotherm

ODSH inhibits the corrosion of mild steel by adsorption on the metal surface. The adsorption provides the information about the interaction between the adsorbed molecules on the metal surface (electrode surface). Adsorption isotherm provides the basic information about the interaction between inhibitor and steel surface [38]. Attempts were made to fit various isotherms including Frumkin, Langmuir and Temkin. The graph drawn with values of C_{inh}/SC vs. C_{inh} (SR-surface coverage) gave a straight line with the approximate unit slope. It indicates that adsorption obeys the Langmuir adsorption isotherm as shown in Fig. 5. Assumptions of Langmuir relate the concentration of the adsorbate in the bulk of the electrolyte (C_{inh}) to the degree of surface coverage (CR) and K_{ads} is the equilibrium constant of adsorption.

$$\frac{C_{inh}}{\theta} = \frac{1}{K_{ads}} + C_{inh} \tag{8}$$

The linear regression coefficient (R^2), the standard free energy of adsorption (ΔG^0_{ads}) and equilibrium constant (K_{ads}) are the parameters obtained from adsorption isotherm:

$$\Delta G^o_{ads} = -RT\ \ln(55.5\ K_{ads}) \tag{9}$$

where 55.5 is the concentration of water in solution in mol L^{-1} and R is the universal gas constant. Calculated values of ΔG^0_{ads} and K_{ads} values are recorded in Table 3.

Table 2 Weight loss values of various temperatures.

Concentration (ppm)	Weight loss (mg cm^{-2})				Corrosion rate (mm y^1)				IE (%)			
	303K	313K	323K	333K	303K	313K	323K	333K	303K	313K	323K	333K
Blank	16.67	18.81	19.70	21.27	39.69	44.78	46.90	50.64	–	–	–	–
50	7.44	9.12	10.21	12.27	17.71	21.71	24.30	28.85	55.36	51.51	48.17	43.01
100	6.01	7.63	8.93	10.23	14.30	18.16	21.26	24.35	63.94	59.43	54.67	51.90
150	4.60	6.15	7.72	9.10	10.95	14.64	18.38	21.66	72.40	67.30	60.81	57.21
200	2.91	4.61	5.91	7.63	6.92	9.90	14.07	18.16	82.54	77.88	70.00	64.12
250	2.22	4.90	5.01	6.70	5.28	9.28	11.92	15.95	86.68	79.26	74.56	68.50
300	1.60	3.21	4.21	5.57	3.80	7.64	10.02	13.26	90.40	82.93	78.62	73.81

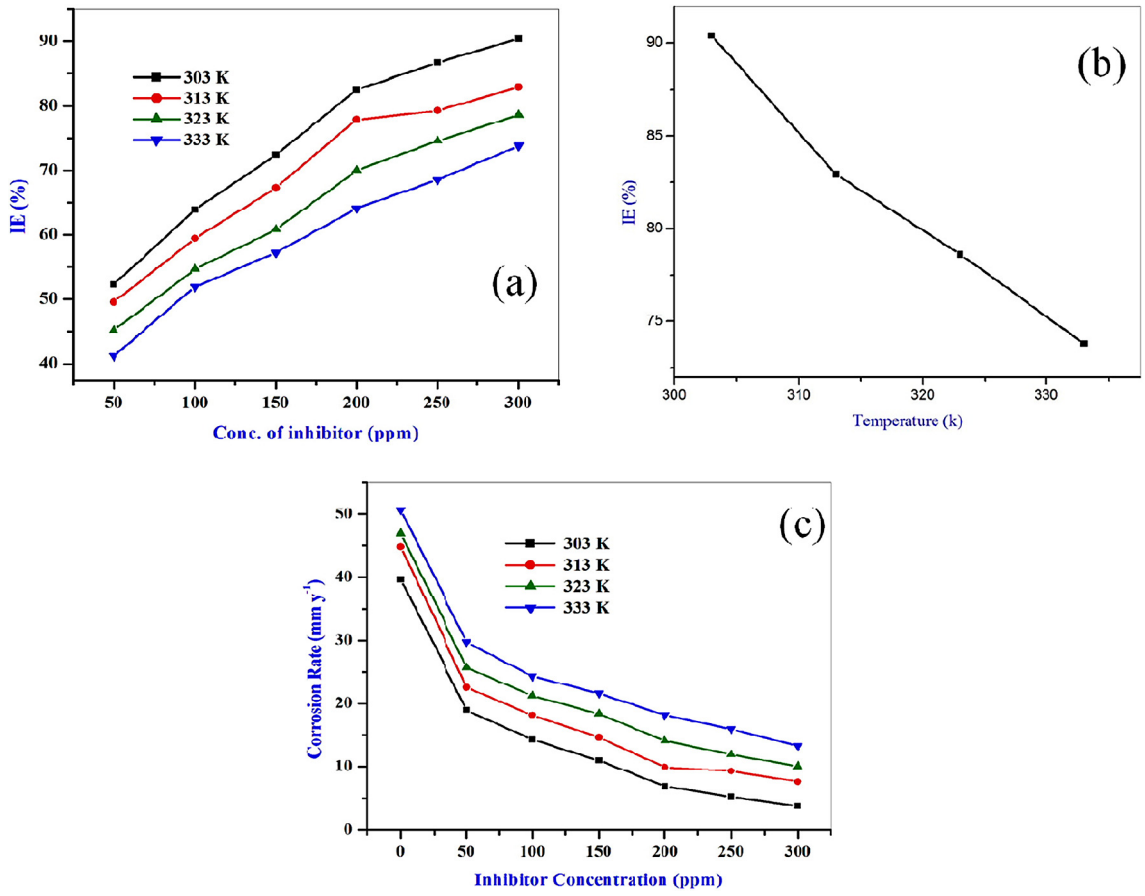

Figure 4 (a) Inhibition efficiency vs various concentrations of inhibitor, (b) inhibitor efficiency vs different temperatures, (c) Corrosion rate vs various concentrations of inhibitor.

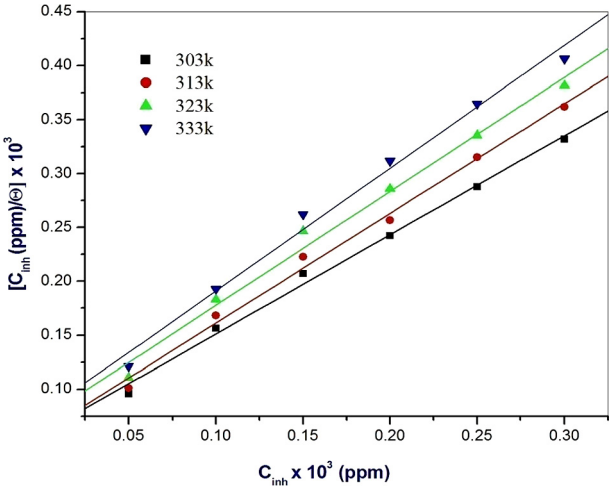

Figure 5 Langmuir adsorption isotherm.

From Table 3 it is known that when the temperature increases ??[2] and K_{ads} values decrease and this is due to adsorbed inhibitor desorbed on the metal surface at a high temperature [39–41]. The above two parameters clearly indicate that adsorption maximum is at a lower temperature and

Table 3 Thermodynamic adsorption parameters for mild steel in 1 M HCl at different temperatures.

Temperature (K)	R^2	K_{ads} ($10^4 m^{-1}$)	$-\Delta G^0_{ads}$ (kj mol^{-1})
303	0.9938	15.3837	17.0359
313	0.9932	14.6106	17.8340
323	0.9888	14.6888	18.0016
333	0.9898	14.7231	18.5654

the result is in good agreement with the value of IE%. The ΔG^0_{ads} values are negative, and the values are −17.0, −17.8, −18.0, and −18.56 kJ/mol corresponding to the temperatures 303 K–333 K, respectively. These values were obtained from the Langmuir isotherm plot. The negative values of ΔG^0_{ads} ensure that the adsorption of the inhibitor molecule onto the steel surface is a spontaneous process. Generally, values of ΔG^0_{ads} up to −20 kJ mol^{-1} are due to physisorption process, while those higher values are due to chemisorption process. This is due to the sharing or transfer of electrons from an inhibitor to the metal surface to form a coordinate type of metal bonds [42]. In the present study, the calculated values of ΔG^0_{ads}, range between −17.0 and −18.5 kJ mol^{-1} (Table 3), which indicates that the ODSH follows the physisorption process at a different temperatures in 1 M HCl.

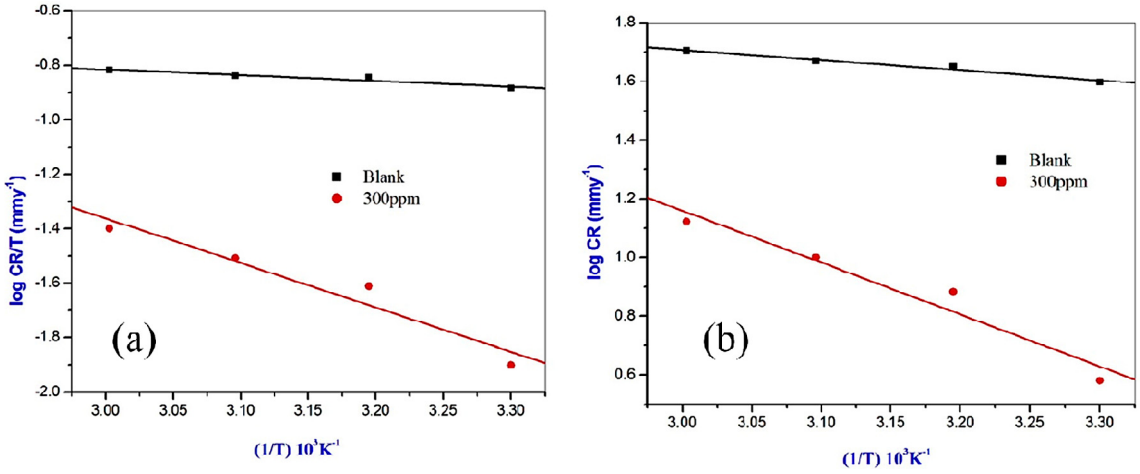

Figure 6 Adsorption isotherm plot: (a) log CR vs $1/T$, (b) log CR/T vs $1/T$.

Table 4 Thermodynamic activation parameters of mild steel in 1 M HCl with and without various concentrations of ODSH.

Concentration (ppm)	E_a^0 (kj mol^1)	ΔH_{ads}^0 (kj mol^{-1})	$-\Delta S_{ads}^0$ (kj mol^{-1})
Blank	6.5502	3.9041	193.7041
Inhibitor	33.9000	31.2519	265.2792

3.1.4. Thermodynamic parameters

Thermodynamic parameters are important to understanding the inhibition mechanism. The thermodynamic functions determined from the dissolution of mild steel with and without the addition of ODSH at various temperatures are calculated from the logarithm of corrosion rate (CR) of metal in 1 M HCl solution using the Arrhenius equation:

$$\log \mathrm{CR} = \frac{-E_a^o}{2.303RT} + A \tag{10}$$

Table 5 Electrochemical impedance parameters of mild steel in 1 M HCl containing different concentrations of ODSH.

Concentration (ppm)	Y_{max} (Ω cm^2)	R_{ct} (Ω cm^2)	C_{dl} (μF cm^2)	IE (%)
Blank	8.050	16.088	1229.5	–
50	18.002	36.109	244.96	55.44
100	24.395	48.936	133.38	67.12
150	32.001	64.339	77.339	74.99
200	45.831	92.422	37.592	82.59
250	64.164	129.865	19.109	87.61
300	70.214	140.752	16.112	88.56

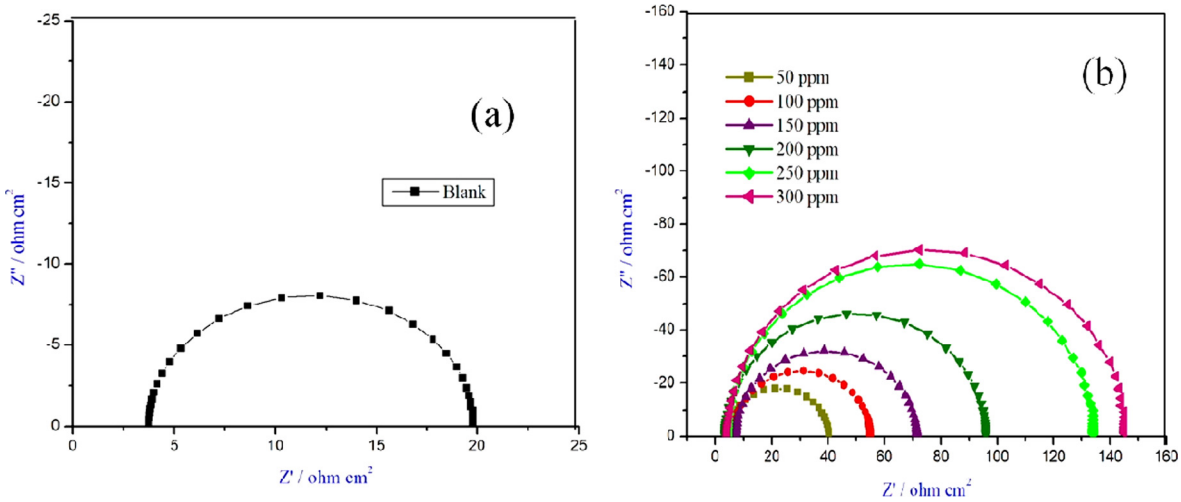

Figure 7 Nyquist plot: (a) blank, (b) various concentrations of ODSH.

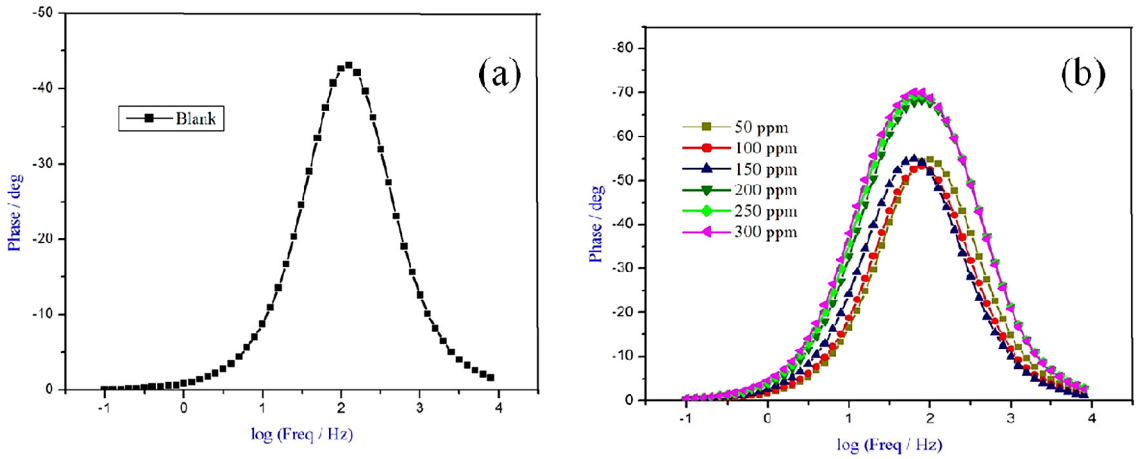

Figure 8 Bode plot: (a) blank, (b) various concentrations of ODSH.

where E_a^0 is the apparent activation energy and A is the pre-exponential factor. The Arrhenius plots of log CR vs $1/T$ for blank and optimum concentrations of ODSH, graph give a straight line a slope equal to $-(E_a^0/2.303R)$ shown in Fig. 6 (a), using the numerical value of the slope, E_a^0 is determined and recorded in Table 4. From the table, $E°_a$ value obtained for the blank is 6.5502 kJ mol^{-1}. In the presence of inhibitor, the activation energy is increased up to 33.9 kJ mol^{-1}. This change may be due to the change in potential difference between metal and solution interface. The change in $E°_a$ suggests that the inhibitor either may participate in the electrode process or may change the potential difference between metal and solution interface. From the transition state equation:

$$CR = \frac{RT}{Nh}\exp\left(\frac{\Delta S_a^o}{R}\right)\exp\left(-\frac{\Delta H_a^o}{RT}\right) \quad (11)$$

where ΔH_{ads}^0 is the enthalpy of activation, ΔS_{ads}^0 is the entropy of activation, h is Planck's constant, N is the Avogadro number and R is the universal gas constant.

The Fig. 6(b) is drawn by plotting log(CR/??) vs 1/?? which gives a straight line with a slope equal to $-(\Delta H_{ads}^0/2.303R)$ and an intercept equal to $(\log(R/Nh) + (\Delta S_{ads}^0/2.303R))$. From these values, the ΔH_{ads}^0 and ΔS_{ads}^0 are calculated and listed in Table 4. The positive signs of $\Delta??_{ads}^0$ refer to the endothermic nature of the mild steel dissolution process, suggesting that the dissolution of mild steel is slow in the presence of inhibitor [45]. The entropy of activation, $\Delta S_{??ds}^0$ in the absence and presence of ODSH is −193.7041 kj mol^{-1} and −265.2792 kj mol^{-1} respectively. This value is large and negative, implying that the rate-determining step for the activated complex is the association rather than the dissociation step [43]. The negative values of ΔS_{ads}^0 might be explained in the following way: before the adsorption of inhibitor onto the metal surface the inhibitor molecules might freely move in the bulk solution, but with the progress in the adsorption the inhibitor molecule was orderly adsorbed onto the metal surface, so there is a decrease in entropy [44].

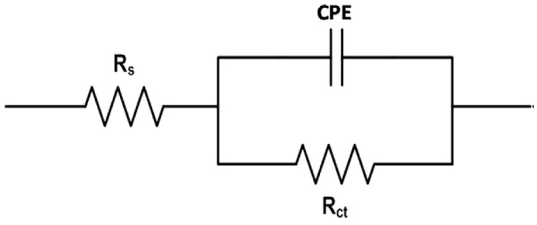

Figure 9 Electrical equivalent circuit model.

3.2. Electrochemical study

3.2.1. Electrochemical impedance spectroscopy

The impedance method provides the information about corrosion inhibition process. The kinetics of the electrode processes and the surface properties of the systems were also investigated by this method. The experimental results obtained from EIS measurements for the corrosion of mild steel in the presence and absence of ODSH at 30 °C are summarized in Table 5. There are two types of impedance spectra. One is Nyquist plots shown in Fig. 7(a) and (b) another one is Bode shown in Fig. 8 (a) and (b). In the Nyquist plots, single semicircle indicates that the charge transfer process takes place at the electrode/solution interface, and the charge transfer process controls corrosion reaction of steel and the presence of inhibitor does not change the mechanism of steel dissolution [45]. In addition, these impedance diagrams are not perfect semicircles, which are related to the frequency dispersion because of the roughness and inhomogeneous of electrode surface [46–49]. Here, CPE is substituted for double-layer capacitance, C_{dl} to give a more accurate fit. Furthermore, the impedance spectra response of mild steel in uninhibited HCl solution has significantly changed after adding the ODSH in HCl solution. As a result, real axis intercepts at high, low frequencies in the presence of inhibitor are bigger than that in the absence of the inhibitor, and the radius of the semicircle increases with increasing inhibitor concentration. This confirms that the impedance increases with increasing ODSH concentration in 1 M HCl.

In the Bode plot, (Fig. 8b) phases are high at high frequencies and it provides a general idea of the anti-corrosion performance of inhibitor. The phase angle increases at the negative direction and it indicates that the inhibitor has electrochemical behavior [50]. In the Bode plot (Fig 8b), the phase angle reaches negative value, at a high frequency, when the concentration of the inhibitor is increased. It indicates good inhibitive behaviors at a high concentration [51]. The equivalent circuit

shown in Fig. 9 simulates the EIS results. It is used to verify the mechanism of the electrochemical process and using this numerical value corresponding to the physical and/or chemical properties of the electrochemical system [52] is calculated. The circuit employed allows the identification of both solution resistance (R_s) and charge transfer resistance (R_{ct}). It is worth mentioning that the double layer capacitance (C_{dl}) value is affected by imperfections of the surface, and this process is simulated via a constant phase element (CPE) [53]. The impedance function of a CPE is defined by the mathematical expression given below

$$Z_{CPE} = [Y_0(j\omega)^n]^{-1} \quad (12)$$

where j is the imaginary root, ω is angular frequency, Y_0 is the magnitude of CPE and n is the exponential term [54]. As can be seen from Table 5, R_{ct} values increased with an increase in the concentration of the inhibitor, indicating a charge transfer process mainly controlling the corrosion of the mild steel. The charge transfer resistance increases, with an increase in the current density on the metal surface, it passes through the capacitor in the electric circuit. The frequency of the imaginary component having maximum impedance ($-Z''_{max}$) was observed and the C_{dl} values were obtained from the following equation:

$$C_{dl} = (2\pi f_{max} R_{ct})^{-1} \quad (13)$$

The values of C_{dl} (Table 5) decreases with an increase in the concentration of the inhibitor, which confirms the increasing level of adsorption of the inhibitor on the metal surface [55]. The adsorption of inhibitor on the mild steel surface may be attributed to the formation of a protective layer and this may be due to the presence of functional groups containing hetero atoms such as 'N' and 'O', which are present in the inhibitor molecules. The decrease in C_{dl} values results from a decrease in local dielectric constant and/or increase in the thickness of the electrical double layer. It also indicates the gradual replacement of water molecules by the adsorption of the inhibitor molecules on the metal surface, decreasing the magnitude of metal dissolution [34]. The thickness of this protective layer δ_{inh} was related to C_{dl} by the following equation [56].

$$\delta_{inh} = \frac{\varepsilon_0 \varepsilon_r}{C_{dl}} \quad (14)$$

where ε_0 is the dielectric constant and ε_r is the relative dielectric constant. From Table 5, it can be seen that the R_{ct} values increased and the values of C_{dl} decreased with an increase in ODSH concentrations. In this situation the surface covered by the inhibitor, which leads to an increase in the IE%. R_{ct} values were used to calculate the IE% and surface coverage (θ) according to the previously mentioned relationship 4 & 5. Table 5 confirms that the IE% increases when the concentration of inhibitor increases and the maximum efficiency of 88.56% reaches 300 ppm. As inhibitor concentration increases, it covers more and more surface area and results in reduction of the corrosion rate. All the above results infer that with the increase in ODSH concentration, the protective film becomes more and more protective.

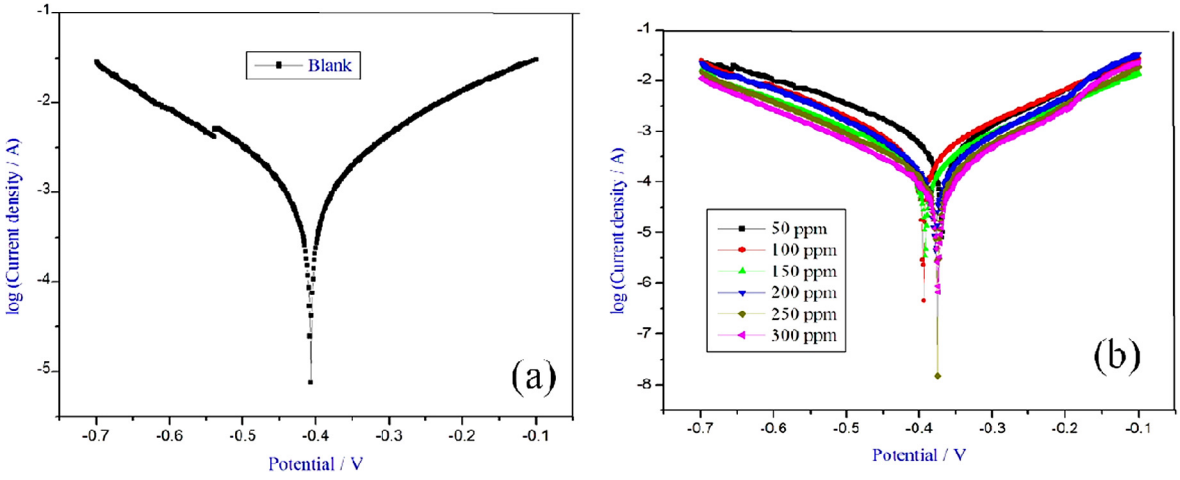

Figure 10 Tafel polarization plot: (a) blank (b) various concentration of ODSH.

Table 6 Tafel polarization parameters of mild steel in 1 M HCl with and without various concentrations of ODSH.

Conc. (ppm)	b_a mV dec^{-1}	b_c mV dec^{-1}	E_{corr} (mV/SCE)	I_{corr} (mA/cm^2)	R (Ohm)	IE (%)
Blank	653.1	651.1	−449.6	1.087	31	–
50	701.5	658.7	−369.1	0.5190	62	52.25
100	720.8	743.5	−388.7	0.3623	82	66.66
150	660.5	764.9	−434.7	0.2928	119	73.06
200	801.7	838.4	−296.0	0.1921	138	82.32
250	730.1	664.9	−297.0	0.1548	201	85.75
300	753.8	724.0	−316.8	0.1024	281	90.57

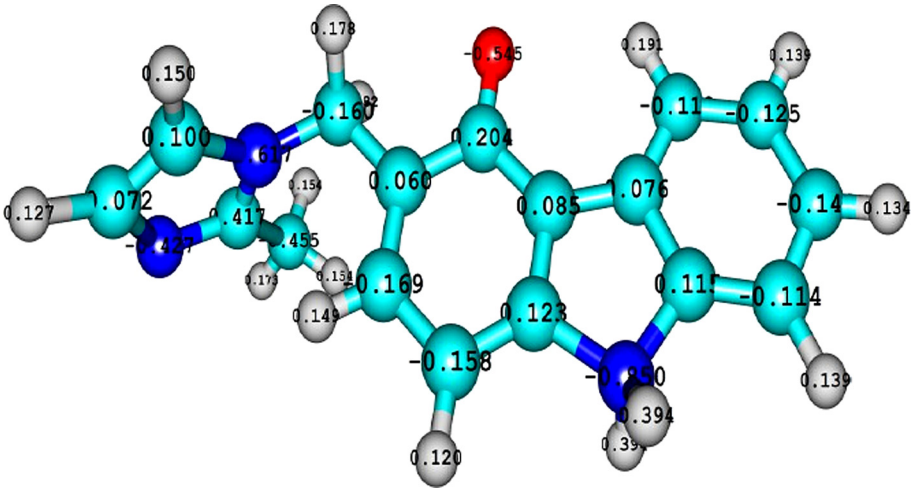

Figure 11 Optimized structure with Mulliken charges.

Table 7 Quantum chemical parameters of ODSH.

E_{HOMO} (eV)	E_{LUMO} (eV)	$\Delta E = (E_{HOMO} - E_{LUMO})$	μ (D)	Total energy (E) (A.U)	IE (%)*
−4.6471	−1.1583	3.4888	12.3624	−896.0249	90.57

* IE (%) values were calculated from Tafel polarization measurements.

3.2.2. Tafel polarization

The polarization curves of mild steel in 1 M HCl with and without various concentrations of ODSH at 30 °C are shown in Fig. 10(a) and (b) respectively. The Tafel polarization method provides information about the type of corrosion inhibitor either anodic or cathodic. The following values obtained from polarization measurements such as corrosion potential (E_{corr}), corrosion current (I_{corr}), anodic and cathodic Tafel slopes (b_a and b_c) are given in Table 6. Inhibition efficiency (IE%) and surface coverage (θ) values were calculated from the previously mentioned relationships 6 & 7.

The polarization results are conformed to the impedance results. It exhibits all corrosion parameters including the inhibition efficiency. The parallel cathodic Tafel lines suggested that the addition of the inhibitor to the 1 M HCl solution does not modify the hydrogen evolution mechanism or the reduction of H^+ ions at the mild steel surface, which occurs mainly through a charge transfer mechanism [57]. The change in the values of cathodic Tafel slope in the presence of inhibitor clearly indicates the effect of the inhibitor compound on the kinetics of hydrogen evolution. The shift in the anodic Tafel slope values may be due to the adsorption of inhibitor molecules onto the mild steel surface [58].

The inhibition studied is suppressing both anodic and cathodic reactions. It is adsorbed on the mild steel surface and blocks the corrosion active sites. These results suggested that the addition of the inhibitor to the 1 M HCl solution reduces the anodic dissolution and retards the cathodic hydrogen evolution reaction, indicating that this inhibitor exhibits both cathodic and anodic inhibition effects [59,60]. Therefore, ODSH can be classified as a mixed inhibitor in 1 M HCl solution. The cathodic and anodic Tafel slope values are almost the same with and without the inhibitor. This confirms that ODSH adsorbs on the metal surface by simply blocking the active sites, and the mechanisms of anodic and cathodic reactions are affected [61]. A compound can be classified as a cathodic or an anodic type inhibitor when the change in E_{corr} value is at least 85 mV in relation to that one measured for the blank

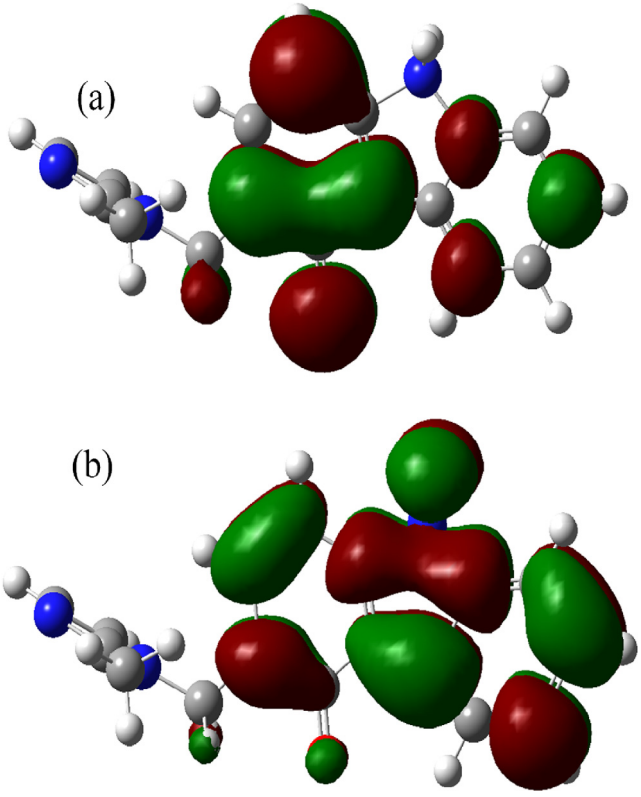

Figure 12 (a) HOMO, (b) LUMO.

solution [62]. However, a shift of corrosion potential (E_{corr}) of ODSH toward the anodic side, i.e. −449.6 to −316.8 mV, was observed. Since the larger displacement exhibited by ODSH is less than the blank (−449.6 mV), it is concluded that the addition of ODSH significantly alters the value of E_{corr} indicating that the added inhibitor is more polarized in the anodic side. The I_{corr} values decrease steadily from the blank value with the increases in inhibitor concentration from 50 to 300 ppm.

Since, the corrosion current is proportional to the magnitude of the corrosion reaction. The decrease in I_{corr} clearly confirms that the inhibition efficiency increases with an increasing ODSH concentration [63]. The polarization resistance (R_P) value increases with increasing concentration of ODSH, which suggests the reduction of mild steel corrosion in the solution with inhibitor compared to the uninhibited solution. ODSH attained maximum inhibition efficiency of 90.57% at 300 ppm in Tafel polarization measurement.

3.3. Quantum chemical calculations

The quantum chemical calculations are powerful tools for studying corrosion inhibition mechanism. Furthermore, the result of quantum chemical calculations could be obtained without laboratory measurements, thus saving time and equipment. There is an increasing number of publications attempting to correlate the structure of corrosion inhibitors. Their state of adsorption at the metal/solution interfaces and inhibition effectiveness are appearing in the literature [46]. Quantum chemical calculation is used to design and develop new corrosion inhibitors using which we can obtain evidence regarding the distribution of electron for different molecular geometries. Parameters such as Highest Occupied Molecular Orbital (HOMO), Lowest Unoccupied Molecular Orbital (LUMO), electron density parameters (dipole moment) and Mulliken charges are considered to analyze the reactivity of the inhibitor. The optimized structure of ODSH is shown in Fig. 11. The computed quantum chemical data are summarized in Table 7 and the structure of HOMO and LUMO are given in Fig. 12(a) and (b). Inhibitor molecule is adsorbed on the metal surface by the donor–acceptor interactions between inhibitor molecules and the metal surface. The highest occupied molecular orbital energy level (E_{HOMO}), as a measure of electron donating ability of a molecule explains the adsorption on metallic surfaces by way of delocalized pair of π-electrons. It related to the electron donating ability of the inhibitor and the electron donating tendency increases with increasing E_{HOMO}. The E_{HOMO} increases the reactivity of molecules and so is easily adsorbed on the metal surface.

The E_{LUMO} relates the ability of a metal/molecule to accept electrons and lower value of E_{LUMO} indicates the easier

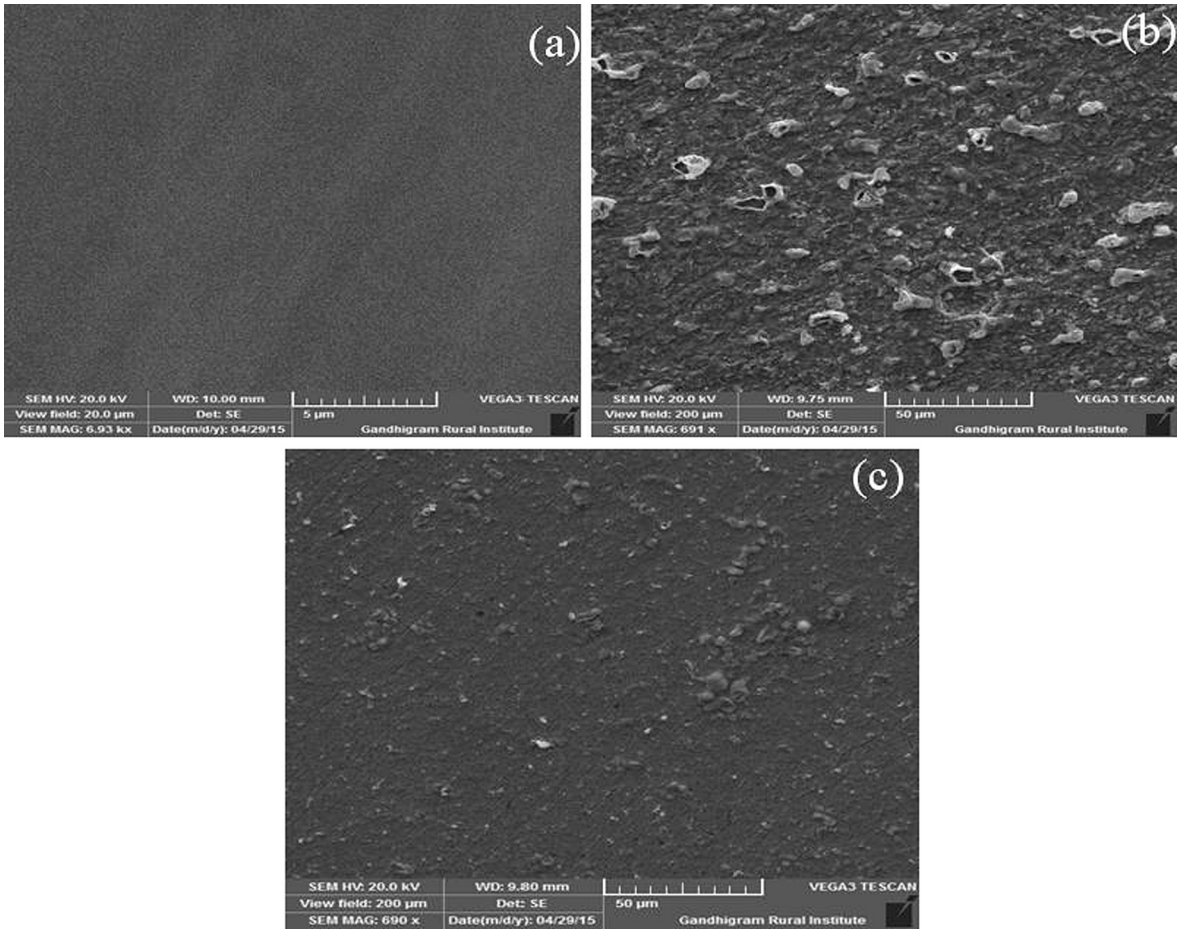

Figure 13 SEM image of mild steel: (a) polished metal, (b) 1 M HCl solution without ODSH (c) 1 M HCl solution with optimum concentration of ODSH.

acceptance of electrons from the metal surface [64]. In the present study shows the value of E_{HOMO} is high compared to E_{LUMO}, which indicates that it easily donates an electron pair from the metal surface to form metal-ligand coordination.

The inhibition efficiency increases with decreasing $E_{HOMO} - E_{LUMO}$ (ΔE) because the excitation energy gap is more polarizable and is generally associated with chemical reactivity [65], so lower ΔE values aid in an electron transfer process between the inhibitor molecules and the mild steel surface. The calculated ΔE value for the ODSH is 3.4888 eV, and it justifies the results. Karthik et al. studied the corrosion inhibition performance of two diaza-adamantane derivatives, and they found ΔE values of 4.3620 and 4.8809 eV for Inhibitor 5,7-diphenyl-1,3-diaza adamantan-6-one (HDDA) and 6-hydroxy-5,7-diphenyl-1,3-diaza adamantine (DDA) respectively, [35]. Nataraj et al. studied a few organic compounds, and they found ΔE values of 8.13, 6.56, and 5.47 EV for 2-[4-(methylthio)phenyl] acetohydrazide (HYD), 2-{[4-(methylthio) phenyl] acetyl} hydrazine carbothioamide (TAD), and 5-[4-(methylthio) benzyl]-4H-1,2,4-triazole-3-thiol (TRD) respectively [66].

The dipole moment gives information on the polarity (the hydrophobicity) of the molecule. When the dipole moment of the molecule increases the absorption of inhibitor also increases on the mild steel surface [24]. The calculated dipole moment (μ) of ODSH is 12.3628.

3.4. Surface studies

3.4.1. Scanning electron microscopy (SEM)

The SEM images were recorded (Fig. 13a–c) to establish the interaction of inhibitor molecules with the metal surface. The SEM images show the features of mild steel surface after 3 h in 1 M HCl in the absence and presence of 300 ppm ODSH at 303 K. The SEM image shows that the mild steel specimen immersed in inhibitor solution is in better conditions, having a smooth surface while the metal surface immersed in blank acid solution is rough, covered with corrosion products and appeared like full of pits and cavities. This indicates the ODSH molecule hinders the dissolution of iron by forming a protective film on mild steel surface and thereby reduces the corrosion rate.

3.4.2. Energy dispersive X-ray spectroscopy (EDX)

An EDX spectrum was recorded for the mild steel sample, which is immersed in 1 M HCl solution with and without concentration of inhibitor. Fig. 14(a) shows the polished metal

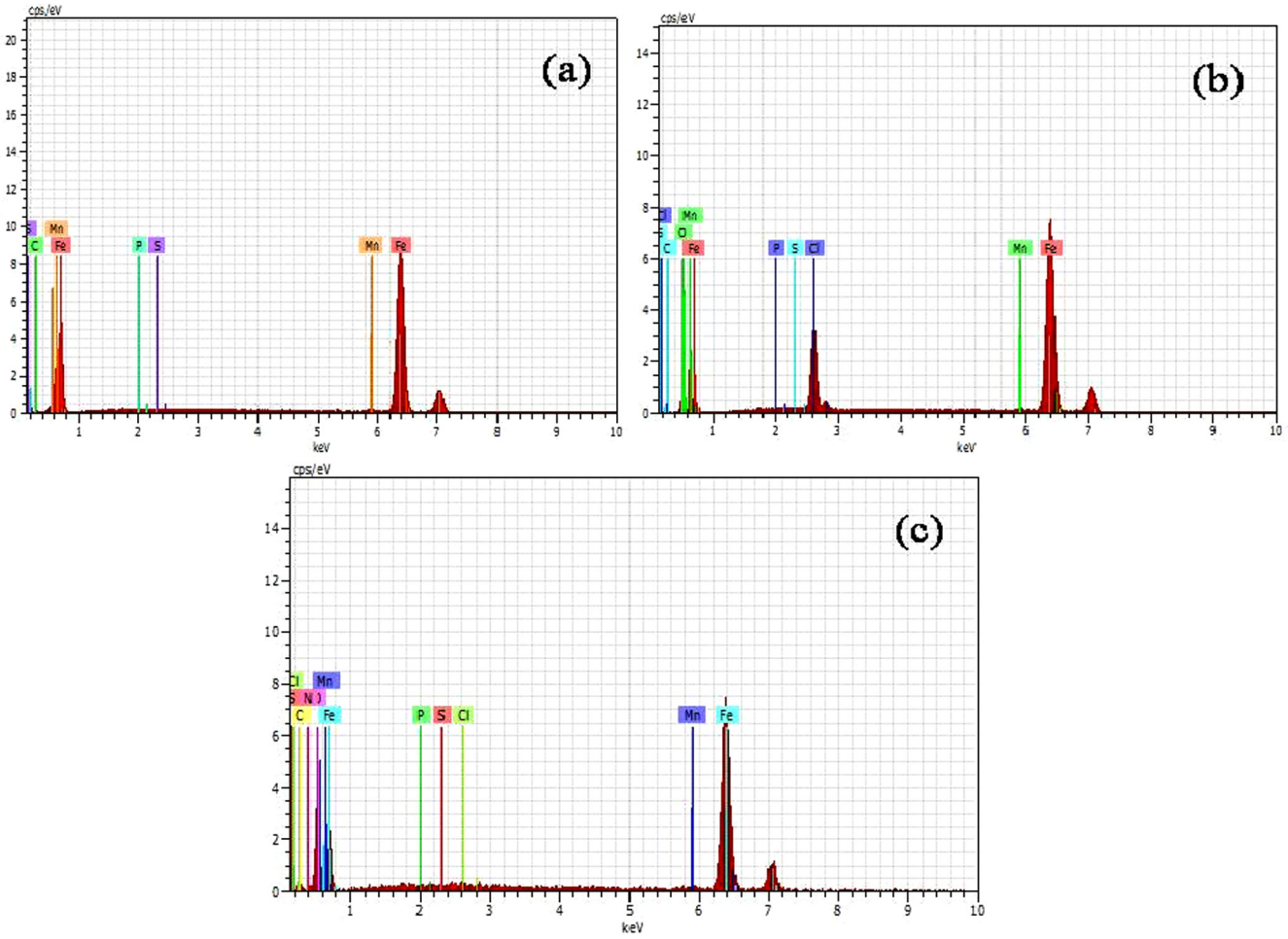

Figure 14 EDX spectrum of mild steel: (a) polished metal, (b) 1 M HCl solution without ODSH, (c) 1 M HCl solution with optimum concentration of ODSH.

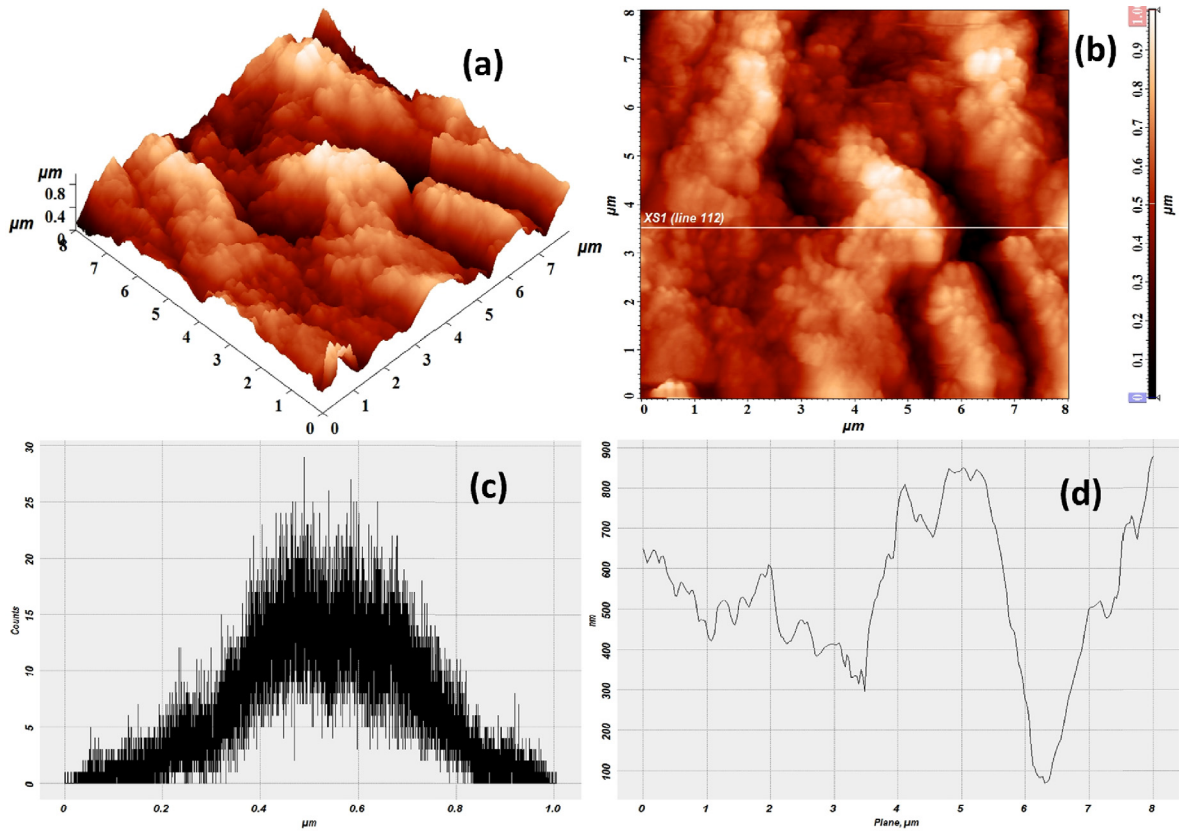

Figure 15 AFM images of mild steel in 1 M HCl solution: (a) 3D, (b) Histogram analysis, (c) 2D and (d) cross section line profile.

Table 8 AFM data for mild steel surface and immersed in with and without ODSH.

Samples	Root mean square roughness (nm)	Maximum peak-to-peak height (nm)	Average roughness (nm)
1 M HCl	169.835	1004.44	136.84
300 ppm inhibitor	25.0328	224.49	19.742

Table 9 FT-IR values of inhibitors and its corresponding protective film formed on mild steel shown.

Group responsible	IR Frequency of pure ODSH (cm^{-1})	Protective film (cm^{-1})
O–H	3344	3397
N–CH_3	2906	2930
C═O	1651	1621
Ar C═C	1432	1315
C–N	1064	1044

surface. This spectrum contains Fe, Mn, S, P, and C. It can be observed that there is no corrosion product present in the polished metal surface and indicate the composition of mild steel composition. In Fig. 14(b) which was recorded without out inhibitor and surface contains chlorine and oxygen. It shows that corrosion product is formed on the metal surface. In Fig. 14(c) with the optimum concentration of inhibitor, the surface contains a nitrogen atom, indicating that inhibition occurs on the metal surface. In the surface chlorine content is decreased which clearly indicated that protective film is formed on the metal surface.

3.4.3. Atomic force microscopy (AFM)

AFM is a powerful technique to investigate the surface morphology of mild steel surface at nano to micro-scale and has become a new choice study on the generation and the progress of the corrosion of the metal/solution interface. The two-dimensional and three-dimensional AFM morphologies for the mild steel surface immersed in 1 M HCl with and without 300 ppm ODSH are shown in Figs. 15 and 16(a–d). The root mean square (rms) and average roughness value carried out for both the protected and unprotected mild steel surface are given in Table 8.

The presence of ODSH in 1 M HCl significantly root mean square roughness reduces to 25.0328 nm, when compared with 169.835 nm for blank. These parameters confirm that the surface appears smoother and the smoothness of the surface is due to the formation of a compact protective film of ODSH on the metal surface, thereby inhibiting the corrosion of mild steel. A uniform variation of the thickness in section analysis also indicates homogeneity of the film.

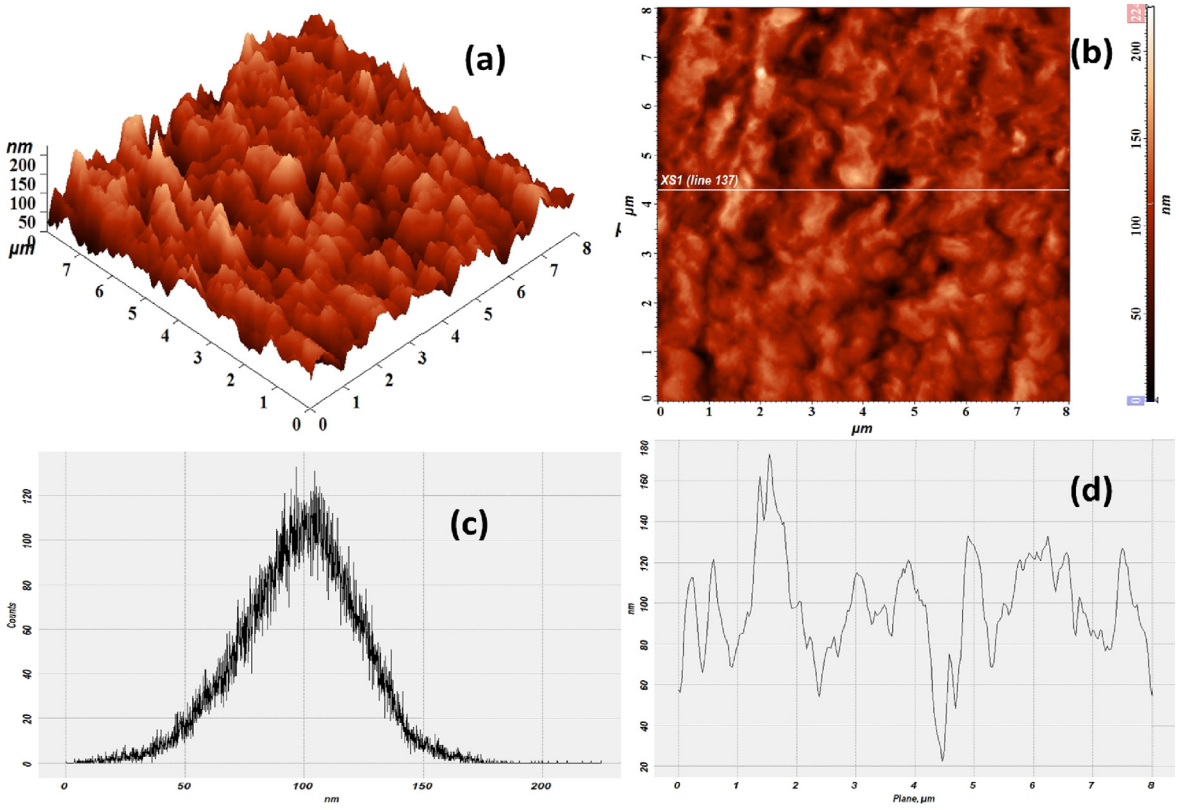

Figure 16 AFM images of mild steel in 1 M HCl solution with optimum concentration of ODSH: (a) 3D, (b) Histogram analysis, (c) 2D and, (d) cross section line profile.

3.4.4. Fourier Transform infrared spectroscopy

The FT-IR values of purity and protective film are shown in Table 9. The IR spectrum of pure ODSH shows lines for N–CH_3, C═O, O–H, C–N and Ar C═C groups at 2906 cm^{-1}, 1651 cm^{-1}, 3344 cm^{-1}, 1064 cm^{-1} and 1432 cm^{-1} respectively. The IR spectrum of protective film N–CH_3, C═O, O–H, C–N, Ar C═C group shows lines at 2930 cm^{-1}, 1621 cm^{-1}, 3397 cm^{-1}, 1044 cm^{-1}, 1315 cm^{-1} respectively. The O–H, N–CH_3 line shifted upward and C═O, Ar C═C, the C–N line shifted downward. It clearly indicates that all the above groups are involved in film formation using a lone pair of electrons and aromatic π electron spectrum as shown in Fig. 17(a) and (b).

3.5. Mechanism of corrosion inhibition

The adsorption of the inhibitor depends on the factors like the chemical composition of the inhibitor, the temperature and electrochemical potential on the metal/solution interface. In fact, the solvent water molecules could also adsorb at a metal/solution interface. Adsorption process can occur through the replacement of solvent molecules from metal surfaces by ions and molecules accumulated near the metal/solution interface [1]. The anions are adsorbed when the metal surface has an excess positive charge in an amount greater than that required to balance the charge corresponding to the applied potential. Aromatic compounds (which contain the π electrons) undergo particularly strong adsorption on many electrode surfaces. The bonding can occur between the metal surface and the aromatic ring. The exact nature of the interactions between a metal surface and an aromatic molecule depends on the relative coordinating strength toward the given metal of the particular groups present [67].

In aqueous acidic solution, ODSH exists either as a neutral molecule or as protonated molecules (cation). One and/or more of the following ways might adsorb ODSH on the metal/acid solution interface. (a) Electrostatic interaction of protonated molecules with already adsorbed chloride ions in the metal surface (b) donor–acceptor interactions between the π-electron of the aromatic ring and vacant d orbital of surface iron atoms, (c) interaction between unshared electron pairs of heteroatom and vacant d-orbital of iron surface atoms. On the various spectral data, we concluded ODSH may be adsorbed on the metal surface in following ways.

ODSH available in the form of hydrochloride, the hydrochloride hydrogen may be stable the ondansetron structure, it accompanies with carbonyl group to form intermolecular hydrogen bonding. FT-IR spectroscopy shows OH stretching frequency appear at 3397 cm^{-1} and carbonyl group stretching frequency appear at 1621 cm^{-1}, it conforms hydroxyl group and carbonyl group presence but in the intensity of CO stretching frequency is weak and lower adsorption value it clearly conforms inter molecular hydrogen bonding presence on the ODSH structure.

On the above discussion, we have concluded ondansetron exists in the protonated form, mild steel immersed in 1 m HCl solution, the chloride ion deposited on the metal surface. This time, mild steel surface becomes negatively charged, this

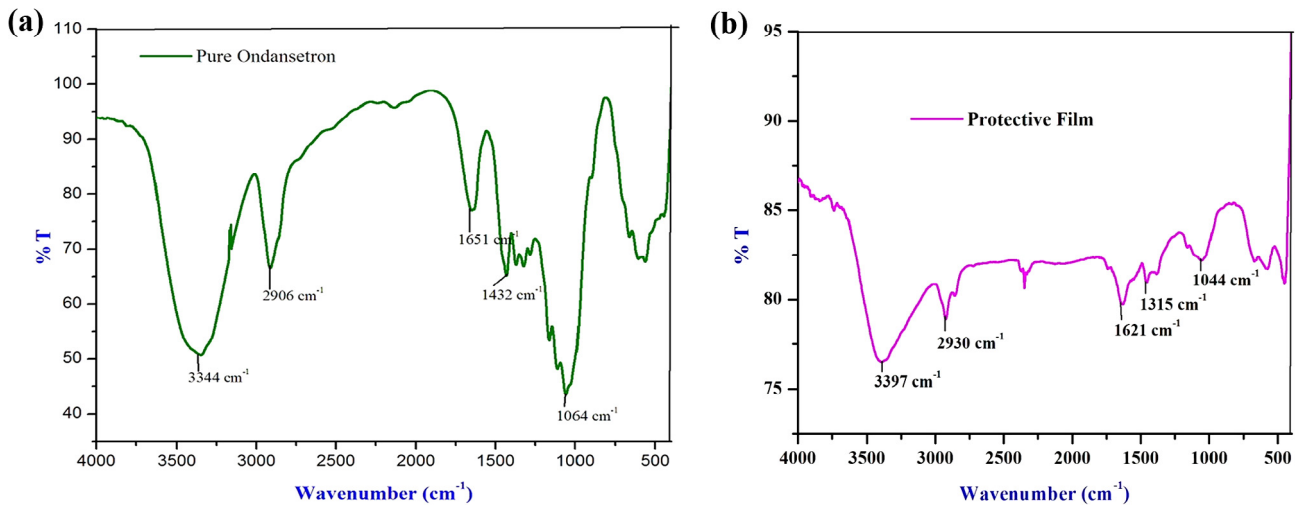

Figure 17 (a) pure ODSH (b) Productive film of mild steel with optimum concentration of ODSH.

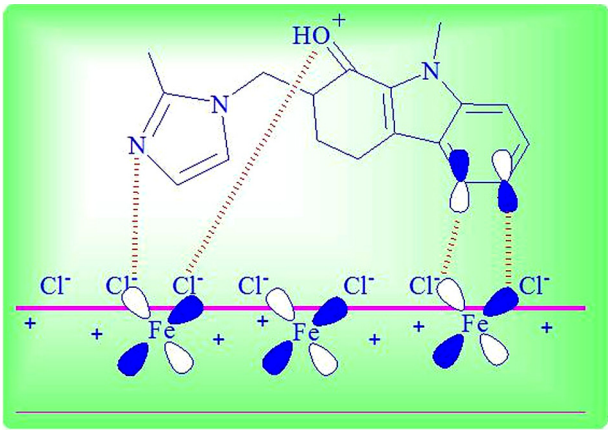

Figure 18 Mechanism of ODSH on the metal surface.

is confirmed by Blank EDX spectrum (chloride content is high on the metal surface). When adding the inhibitor the positively charged oxygen interacts with negatively charged chloride ion to form a strong interaction this interaction is called electrostatic interaction or physical adsorption, it is confirmed by standard free energy value. The aromatic π electrons also interact with the metal surface to form strong interaction, mechanism is clearly shown in Fig. 18.

4. Conclusion

Based on the above results the following conclusions are drawn.

- The results obtained lead to a conclusion that ODSH effectively inhibits the corrosion of mild steel in 1 M HCl solution.
- The inhibition efficiency of mild steel increases with the increase in the ODSH concentrations and with an increase in temperature, the IE% decreases. It shows that corrosion process was inhibited by adsorption of the inhibitor molecule on the mild steel surface.
- The adsorption mode obeys the Langmuir isotherm. The negative values of ΔG^0_{ads} indicate that the adsorption of the inhibitor molecule is a spontaneous process and the adsorption mechanism is physisorption process.
- Tafel curves demonstrated that the ODSH is a mixed-type of inhibitor for mild steel corrosion in 1 M HCl solution. EIS measurements confirm that as inhibitor concentration increases, the charge transfer resistance increases. This shows that the inhibitor performance depends on adsorption of the molecules on the metal surface.
- Quantum chemical calculation is used to confirm the inhibition efficiency of mild steel in 1 M HCl. The inhibition efficiency increases with increasing E_{HOMO} and decreasing ΔE.
- The SEM, AFM images, and EDX, FT-IR spectrum confirm the formation of the protective layer on the mild steel surface.

Acknowledgements

All the above authors are thankful to the university grand commission (UGC) for major research project (MRP) and one of the authors G. Karthik thankful to the university grand commission (UGC) for assistance through basic science research fellowship (BSR).

References

[1] Ishtiaque Ahamad, Rajendra Prasad, M.A. Quraishi, Corros. Sci. 52 (2010) 3033–3041.
[2] M. Lebrini, F. Robert, H. Vezin, C. Roos, Corros. Sci. 52 (2010) 3367–3376.
[3] M. Abdallah, H.E. Meghed, M. Sobhi, Mater. Chem. Phys. 118 (2009) 111–117.
[4] M. Abdallah, E.A. Helal, A.S. Fouda, Corros. Sci. 48 (2006) 1639–1654.
[5] M.G. Hosseini, M. Ehteshamzadeh, T. Shahrabi, Electrochim. Acta 52 (2007) 3680–3685.
[6] B. Obat, N.O. Obi-Egbedi, Corros. Sci. 52 (2010) 198–204.
[7] L. Wang, Corros. Sci. 48 (2006) 608–616.
[8] M. Bouklah, B. Hammouti, M. Lagrenee, F. Bentiss, Corros. Sci. 48 (2006) 2831–2842.

[9] M. Athar, H. Ali, M.A. Quraishi, Br. Corros. 37 (2002) 155–158.
[10] M. Bouklah, A. Ouassini, B. Hammouti, A. ElIdrissi, Appl. Surf. Sci. 252 (2006) 2178–2185.
[11] I. Dehri, M. Ozcan, Mater. Chem. Phys. 98 (2006) 316–323.
[12] A.S. Fouda, A.A. Al-Sarawy, E.E. El-Katari, Desalination 201 (2006).
[13] M. Ajmal, A.S. Mideen, M.A. Quraishi, Corros. Sci. 3 (1994) 79–84.
[14] M. El Achouri, M.R. Infante, F. Izquierdo, S. Kertit, H.M. Gouttoya, B. Nciri, Corros. Sci. 43 (2001) 19–35.
[15] S.S. Abd El-Rehim, M.A.M. Ibrahim, K.F. Khalid, J. Appl. Electrochem. 29 (1999) 593–599.
[16] M. Bethencourt, F.J. Botana, J.J. Calvino, M. Marcos, Corros. Sci. 40 (1998) 1803–1819.
[17] I. Ahamad, M.A. Quraishi, Corros. Sci. 51 (2009) 2006–2013.
[18] A. Chetouani, B. Hammouti, T. Benhadda, M. Daoudi, Appl. Surf. Sci. 249 (2005) 375–385.
[19] J.Z. Ai, X.P. Guo, J.E. Qu, Z.Y. Chen, J.S. Zheng, Colloid. Surface Physicochem. Eng. Aspect. 281 (2006) 147–155.
[20] M.S. Morad, Corros. Sci. 50 (2008) 436–448.
[21] I.B. Obot, N.O. Obi-Egbedi, S.A. Umoren, Corros. Sci. 51 (2009) 1868–1875.
[22] Sudhis Kumar Shukla, M.A. Quraishi, Corros. Sci. 51 (2009) 1007–1011.
[23] Sudhish Kumar Shukla, M.A. Quraishi, Mater. Chem. Phys. 120 (2010) 142–147.
[24] Prasanna B. Matad, Praveen B. Mokshanatha, Narayana. Hebbar, Venkatarangaiah T. Venkatesha, Ind. Eng. Chem. Res. 53 (2014) 8436–8444.
[25] M. Abdallah, Corros. Sci. 44 (2002) 717–728.
[26] R.A. Prabhu, A.V. Shanbhag, T.V. Venkatesha, J. Appl. Electrochem. 37 (2007) 491–497.
[27] M.M. El-Naggar, Corros. Sci. 49 (2007) 2226–2236.
[28] Sudhish Kumar Shukla, Ashish Kumar Singh, Ishtiaque Ahamad, M.A. Quraishi, Mater. Lett. 63 (2009) 819–822.
[29] Ashish Kumar Singh, M.A. Quraishi, Corros. Sci. 52 (2010) 152–160.
[30] Ishtiaque Ahamad, M.A. Quraishi, Corros. Sci. 52 (2010) 651–656.
[31] Nnabuk O. Eddy, Eno E. Ebenso, Int. J. Electrochem. Sci. 5 (2010) 731–750.
[32] Imran Naqvi, A.R. Saleemi, S. Naveed, Int. J. Electrochem. Sci. 6 (2011) 146–161.
[33] G. Karthik, M. Sundaravadivelu, Hindawi Publishing Corporation, ISRN Electrochem. (2013) Doi:10.1155/2013/403542.
[34] G. Karthik, M. Sundaravadivelu, P. Rajkumar, M. Manikandan, Res. Chem. Intermed. 41 (2015) 7593–7615.
[35] G. Karthik, M. Sundaravadivelu, Egypt. J. Petrol. (2015), http://dx.doi.org/10.1016/j.ejpe.2015.04.003.
[36] I.B. Obot, N.O. Obi-Egbedi, Corros. Sci. 52 (2010) 198–204.
[37] Tianpei Zhao, Mu. Guannan, Corros. Sci. 41 (1999) 1937–1944.
[38] Xianghong Li, Shuduan Deng, Corros. Sci. 51 (2009) 1344–1355.
[39] Waheed A. Badawy, Khaled M. Ismail, Ahlam M. Fathi, Electrochim. Acta 51 (2006) 4182–4189.
[40] M.A. Migahed, H.M. Mohamed, A.M. Al-Sabagh, Mater. Chem. Phys. 80 (2003) 169–175.
[41] A.A. Abdul Azim, L.A. Shalaby, H. Abbas, Corros. Sci. 14 (1974) 21–24.
[42] Mirghasem Hosseini, Stijn F.L. Mertens, Mohammed R. Arshadi, Corros. Sci. 45 (2003) 1473–1489.
[43] Gamal K. Gomma, Mostafa H. Wahdan, Mater. Chem. Phys. 39 (1995) 209–213.
[44] Xianghong Li, Mu Guannan, Appl. Surf. Sci. 252 (2005) 1254–1265.
[45] L. Larabi, Y. Harek, M. Traisnel, A. Mansri, J. Appl. Electrochem. 34 (2004) 833–839.
[46] M. Lebrini, M. Lagrenée, H. Vezin, M. Traisnel, F. Bentiss, Corros. Sci. 49 (2007) 2254–2269.
[47] Hong Shih, Corros. Sci. 29 (1989) 1235–1240.
[48] M. Metikos-Hukovic, S. Martinez, J. Appl. Electrochem. 33 (2003) 1137–1142.
[49] M. Elayyachy, A. El Idrissi, B. Hammouti, Corros. Sci. 48 (2006) 2470–2479.
[50] M. Mahdavian, M.M. Attar, Corros. Sci. 48 (2006) 4152–4157.
[51] M. Mahdavian, S. Ashhari, Electrochim. Acta 55 (2010) 1720–1724.
[52] A.R. Sathiya Priya, V.S. Muralidharan, A. Subramania, Corros. Sci. 64 (2008) 541–552.
[53] M. Behpour, S.M. Ghoreishi, N. Mohammadi, N. Soltani, M. Salavati-Niasari, Corros. Sci. 52 (2010) 4046–4057.
[54] Juantao Zhang, Jun Zhao, Ningsheng Zhang, Qu Chengtun, Xiang Zhang, Ind. Eng. Chem. Res. 50 (2011) 7264–7272.
[55] A.V. Shanbhag, T.V. Venkatesha, R.A. Prabhu, J. Appl. Electrochem. 38 (2008) 279–287.
[56] Hamdy H. Hassan, Electrochim. Acta 51 (2006) 5966–5972.
[57] S. Kertit, B. Hammouti, Appl. Surf. Sci. 93 (1996) 59–66.
[58] E. Mc Cafferty, Norman Hockerman, J. Electrochem. Soc. 119 (1972) 146–154.
[59] O. Olivares, N.V. Likhanova, B. Gómez, J. Navarrete, M.E. Llanos-Serrano, E. Arce, J.M. Hallen, Appl. Surf. Sci. 252 (2006) 2894–2909.
[60] H. Ashassi-Sorkhabi, M.R. Majidi, K. Seyyedi, Appl. Surf. Sci. 225 (2004) 176–185.
[61] C. Cao, Corros. Sci. 38 (1996) 2073–2082.
[62] Wei-hua Li, Qiao He, Sheng-tao Zhang, Chang-ling Pei, Bao-rong Hou, J. Appl. Electrochem. 38 (2008) 289–295.
[63] C.N. Cao, Corrosion Electrochemistry Mechanism, 235, Chemical Industrial Engineering Press, Beijing, 2004.
[64] Guan Nan Mu, Xueming Li, Fei Li, Mater. Chem. Phys. 86 (2004) 59–68.
[65] Gopal Ji, Sudhish Kumar Shukla, Priyanka Dwivedi, Shanthi Sundaram, Ind. Eng. Chem. Res. 50 (2011) 11954–11959.
[66] S.E. Nataraja, T.V. Venkatesha, K. Manjunatha, Boja Poojary, M.K. Pavithra, H.C. Tandon, Corros. Sci. 53 (2011) 2651–2659.
[67] I.M. Ritchie, S. Bailey, R. Woods, Adv. Colloid Interface Sci. 80 (1999) 183–231.

Please cite this article in press as: G. Vengatesh et al., A comprehensive study of ondansetron hydrochloride drug as a green corrosion inhibitor for mild steel in 1 M HCl medium, Egypt. J. Petrol. (2016), http://dx.doi.org/10.1016/j.ejpe.2016.10.011